AD-A134 114   APPLICATIONS OF JOSEPHSON JUNCTION SQUIDS AND ARRAYS   1/1
              (U) TRW SPACE AND TECHNOLOGY GROUP REDONDO BEACH CA
              APPLIED TECHNOLOGY DIV   A H SILVER 31 MAR 83
UNCLASSIFIED N00014-81-C-0615   F/G 9/5   NL

END
FILMED
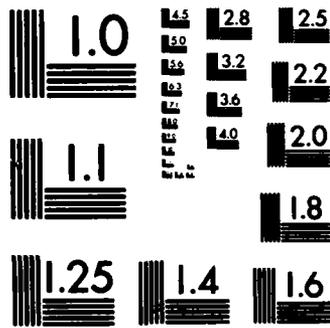
MICROCOPY RESOLUTION TEST CHART
NATIONAL BUREAU OF STANDARDS-1963-A

TRW

A

QUARTERLY PROGRESS REPORT

TO THE

OFFICE OF NAVAL RESEARCH
CODE 414
800 N. QUINCY STREET
ARLINGTON, VA 22217

ON

APPLICATIONS OF JOSEPHSON
JUNCTION SQUIDS AND ARRAYS

CONTRACT NO. N00014-81-C-0615
OCTOBER 1982 - FEBRUARY 1983

PREPARED BY

A.H. SILVER
ADVANCED PRODUCTS LABORATORY

31 MARCH, 1983

A

TRW Inc.

83 10 0 002

INTRODUCTION

This report covers the period from 1 October 1982 to 28 February
1983 following the period covered by the last annual progress
report. This period included the preparation and submission of
the draft of the annual report, presentation of the paper 'SQUID
Voltage-Controlled-Oscillator' to the 1982 Applied Superconduc-
ductivity Conference, continued fabrication and measurement of
the 9GHz SQUID VCO, and design of the dc SQUID and SQUID array
configuration. In addition, a number of important additions and
modifications were made in the basic laboratory facilities.

PROGRESS

Work has continued on fabrication and measurements of the single
resistive SQUID VCO with the 50/1 transformer ratio operating
near 9GHz. Four chips are fabricated on a wafer, with different
damping resistors for each one of the four devices. Figure 1
shows completed devices in an optical photograph of SQUID VCO #3
and 4; wire-bonded leads are shown on #3 for the bias current
leads. Two devices are on each chip. Figure 2 shows VCO #3
mounted in the microwave holder with leads wire-bonded. This
device is placed at the end of a microwave probe with a cooled
circulator connected to one device and a coaxial lead connected
to the other as shown in Figure 3. This coaxial line then goes
directly to room temperature. Either the circulator-coupled VCO
or the coaxial line can then be connected to a low noise X-band
GaAs FET amplifier, followed by a spectrum analyzer. Room
temperature isolators were required between the amplifier and the
spectrum analyzer to eliminate disturbances from the local
oscillator in the analyzer.

Figure 4 shows some output spectra from the VCO as traced from
the spectrum analyzer. Each curve is for a different bias
current and hence dc voltage. Resistances on these devices were
about 50m ohms, which is at least 50 times larger than desired.
Newer fabrication runs are now yielding bias resistance values
near 1mohm, but these devices have not been tested at microwave
frequencies yet. Figure 5 shows the measured I-V curve for one
device. This characteristic results from the parallel combination
of the usual hysteretic junction and a 60mohm resistor, and has
a microbridge-like curve. The critical current is about 75
microamps, compared to the design value of 67 microamps. From
the slope of the linear region we can measure the bias resistance
value. The noise resolution of the measuring system is about 1
microvolt as seen in the measured curve; for more precise
measurements of the dc voltage in determining the tracking of the
VCO, we used a Keithley nanovoltmeter. One can notice some
structure on the I-V curves at a voltage of 47 microvolts,
corresponding to a frequency of about 23 MHz. This may result
from some resonance in the chip structure, but its origin has not
been determined.

The power spectra of Figure 4 are plotted on a linear scale. The

1

peak values are about -100dBm, including 30dB gain the the GaAs
FET amplifier. This represents 10^{-13}W peak power measured with
300 kHz bandwidth on the spectrum analyzer. The oberved spectral
bandwidth is approximately 30 MHz, or a factor of 10^2 times the
detection bandwidth. On the basis of a simple scaling ratio of
this factor, the integrated spectral power is about 10^{-11}W. This
is two orders of magnitude less than expected for these devices.
Some other features of this data are the baseline response of the
spectrum analyzer receiving system which is shown in the center
of the graph in Figure 4. These periodic responses observed with
no current to the VCO have about a 100 MHz period. The origin of
this is not determined. Also the observed spectral amplitudes do
not track smoothly as the voltage across the device is varied.
There is some evidence of this on Figure 4, although it is hard
to demonstrate in a single static picture. The amplitude of the
response varies significantly as the voltage varies, and the
lineshape also varies, including additional structure as seen in
some of the spectra in the figure. In some cases the response
covers a very large bandwidth and may even be multiple valued.

The full explanation is not known, but some comments can be made
at this time. The measured response is that filtered through the
50/1 transformer/filter which may have some unexpected bandpass
and impedance characteristics. For the values of beta and Q
chosen, the VCO should be well-behaved. However, if the
fabrication (or design) were incorrect, and particularly the
reflected impedance from the transformer were not 1 ohm, the
VCO behavior could be significantly changed from the ideal. This
refers to spectral purity, harmonic and subharmonic content, and
even anharmonic behavior as recently reported.[1] For the measured
value of the bias resistance, 60mohm, the predicted value of the
Johnson-noise-limited linewidth is $4.3 \times 10^7 rT$, which at 4K is
10MHz. This is about 3x smaller than the observed value. A
second factor is the influence of external noise on the VCO.
When the VCO is directly connected to the GaAs FET amplifier at
room temperature, the SQUID is subjected to 300K noise filtered
only through the same 50/1 transformer. This could easily cause
serious disturbances of the oscillator as seen from the noise
analysis of a SQUID parametric amplifier[2] of very similar design
and parameter values. One would expect this effect to be
strongly attenuated with a cooled circulator with a cold load;
however, the results of testing the circulator displayed strong
resonances which we could not explain.

----

1. A. H. Silver, R. D. Sandell and J. Z. Wilcox, "SQUID Voltage-
    Controlled Oscillator", IEEE Trans. Magn. MAG-19 (in press)
    (1983).

2. A. H. Silver, R. D. Sandell, J. P. Hurrell and D. C.
    Pridmore-Brown, "SQUID Parametric Amplifier", IEEE Trans.
    Magn. MAG-19 (in press) (1983).

We have studied the problem of designing experiments for the dc
SQUID, dc SQUID pair, and dc SQUID arrays. Particularly, we were
seeking a design which would be adaptable to this expanding set
of devices and experiments without a major change in layout and
coupling method. This problem is more acute with the SQUID
arrays because the junctions are neither connected directly
together nor to a common ground. We plan to fabricate both the
voltage-clamped dc SQUID and SQUID pair on the same wafer using
the geometry shown in Figure 6. This should provide very close
coupling to the oscillating circulating currents in the SQUID
without upsetting the symmetry of the SQUID and with only 3
superconducting films. The voltage clamped dc SQUID pair shown
in Figure 7 can be fabricated with similar coupling geometry. In
this design the voltage-clamping resistor is placed outside the
SQUID itself, and is similar to a dc SQUID pair and a resistive
SQUID tightly coupled with common junctions.

The design for the dc SQUID pair is obviously extendable to the
linear longitudinal array with no change in layout or coupling
method. For the transverse array, one needs a somewhat different
geometry. Figure 8 shows the proposed layout geometry for this
array. This requires that the inductors be located both above
and below the junctions to which they are connected. Each
inductor in the array can be fabricated out of two symmetrically
placed inductors, thereby lowering the total inductance (which is
desirable) and also reducing susceptibility to stray magnetic
fields in the plane of the array and oriented along the line of
the junctions. This design has the desirable feature of minimum
inductance between the various junctions which are directly
connected in the equivalent circuit.

PUBLICATIONS AND PRESENTATIONS

During this reporting period we completed the Annual Progress
Report for this project and presented the paper "SQUID Voltage-
Controlled-Oscillator" to the 1982 Applied Superconductivity
Conference. The text of that paper was submitted for the
Conference Proceedings which will be published in the IEEE
Transactions on Magnetics in 1983. A copy of that paper is
attached to this report.

RELATED ACTIVITIES

A number of related activities of importance to this project are
being carried out in this laboratory, other contractual work and
work sponsored by TRW under IR&D. Two other Navy supported
contracts are:

    Demonstration of SQUID Parametric Amplifier
    Contract No. N00014-81-C-2495
    funded by Naval Research Laboratory

3

SQUID Analog-to-Digital Converter
Contract No. N00014-82-C-0397
funded by Office of Naval Research

It appears very likely that the SQUID VCO techniques being
developed under this project will be useful in supplying an
on-chip clock for the analog-to-digital converter and an
integrated pump for the SQUID low noise parametric amplifier,
particularly at the higher microwave and millimeter wave
frequencies.

TRW is supporting Independent Research and Development to develop
a complete integrated circuit fabrication process for Josephson
technology based on Nb metallization and all Nb junctions, and in
providing satisfactory facilities for circuit design, simulation,
fabrication and testing. A second IR&D project is devoted to
development of millimeter wave imaging systems using Josephson
quasipartical detectors. A four-frequency radiometer using
quasipartical detectors in the incoherent video mode is being
developed for the Naval Research Laboratory flight experiment
measurement program. In addition, TRW is actively exploring the
development of small-scale cryocoolers for deployment of super-
conducting electronics systems, including in-house work on
miniature compressors and discussions of potential collaborations
with J. E. Zimmerman of the National Bureau of Standards and R.
Longsworth and W. E. Steyert of Air Products.

Improvement in the TRW capability to design, simulate, fabricate
and test superconducting integrated circuitry has been proceeding
along several fronts. We have acquired a stand-alone, dedicated,
computer-aided design system for production of mask artwork. The
basic machine was purchased at the end of 1982, and a compatible
magnetic tape generating capability is being acquired this
spring. This will reduce the lead time for mask generation by
several weeks. Several members of the project staff have been
trained in the use of this system.

A Cambridge 100 scanning electron microscope was ordered and will
be delivered during the second quarter of 1983. This machine
will be available full time to the Josephson activities for
sample diagnostics and will also be capable of direct e-beam
pattern generation over a limited field-of-view.

We have acquired, from the Josephson group at UC Berkeley, the
circuit simulation package SPICE, including the Josephson model.
This has now been installed on a time-sharing VAX at TRW and
provides transient response of complex circuits incorporating
Josephson and quasipartical junctions. We plan to utilize this
capability to predict the transient response of the SQUID arrays.

The circuit fabrication laboratory is scheduled for a major
renovation this spring which will improve the air quality,
humidity and temperature control, and water quality. In

4

addition, we plan to install an all-Nb junction process later
this year. The laboratory renovation, acquisition of the CAD
station and SEM, and installation of the Nb junction process
represent a substantial capital investment by TRW in addition to
the IR&D funding.

PLANS

During the next quarter we plan to continue with fabrication and
measurements of the resistive SQUID VCO, and layout and order the
masks for the dc SQUID and SQUID pair VCO. Because of problems
we have experienced with measurements of the VCO, we intend to
fabricate a new microwave probe using only coaxial lines and
cooled coaxial circulators. We hope this will eliminate some of
the observed resonances and the potential for room temperature
noise to interact with the SQUID. For this purpose we have
ordered new cooled coaxial circulators from P&H Labs; delivery is
expected in March/April 1983. This new probe will also be fit to
a 28L superinsulation dewar which has recently been fitted with
high permeability and superconducting shields. This probe will
permit turn-around time reduction of several days compared to
that required for the large waveguide probe presently used.
Also, this will permit the sample to be cooled in milligauss
fields, rather than the earth's field, and should have much lower
stray fields from the magnets in the circulators. (The present
waveguide circulator has an electromagnet with several gauss
stray field at the sample position and associated 60Hz ripple
from both power supply and stray pickup). This probe will be
used for both this contract and the parametric amplifier project
with NRL.

The generation of the dc SQUID masks has been delayed by the
acquisition of the CAD system which should be fully operational
in April. After a test mask set is submitted to a mask house and
is checked out, we will complete the new mask layout and order
the masks. Because of possible stability problems with the
present VCO designs, we may include a new single SQUID design on
the new wafers. Within the present chip design, we can
accommodate up to eight different devices on one wafer.
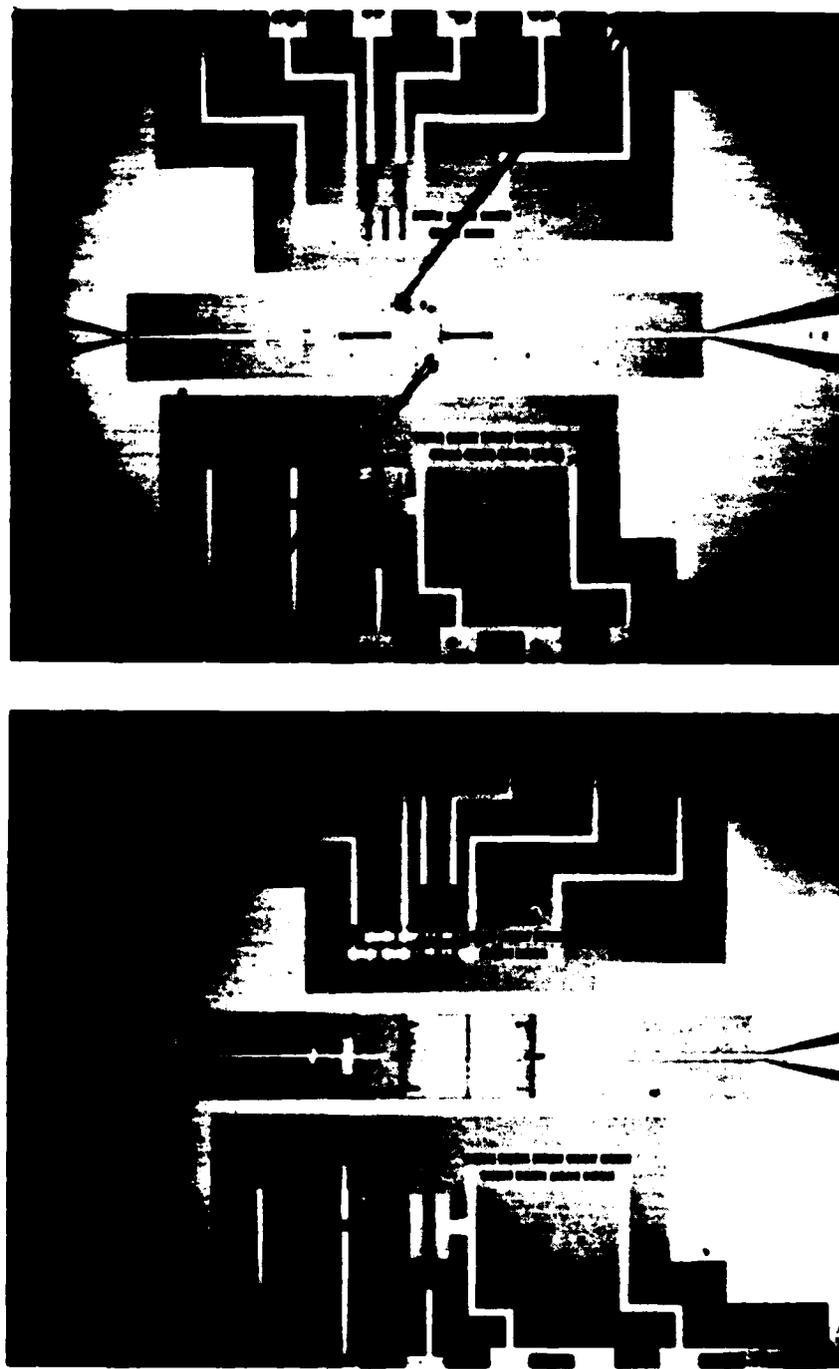
Figure 1. Photographs of the fabricated chips of SQUID voltage-controlled-oscillators #3 (upper photo) and #4 (lower photo). Only the center section of each chip is shown, with two identical devices connected to the 50/1 transformers, which are then coupled to 50 ohm coplanar lines. In the upper photo, the SQUIDs are in-line with a damping resistor off to one side of the microstrip. Wire-bonded leads are shown connected to the bias resistor pad. The structures above and below the VCO are test devices. In #4, the SQUID is transverse to the transmission line and is a figure 8 SQUID with two bias resistors. The damping resistor is in-line with the microstripline.
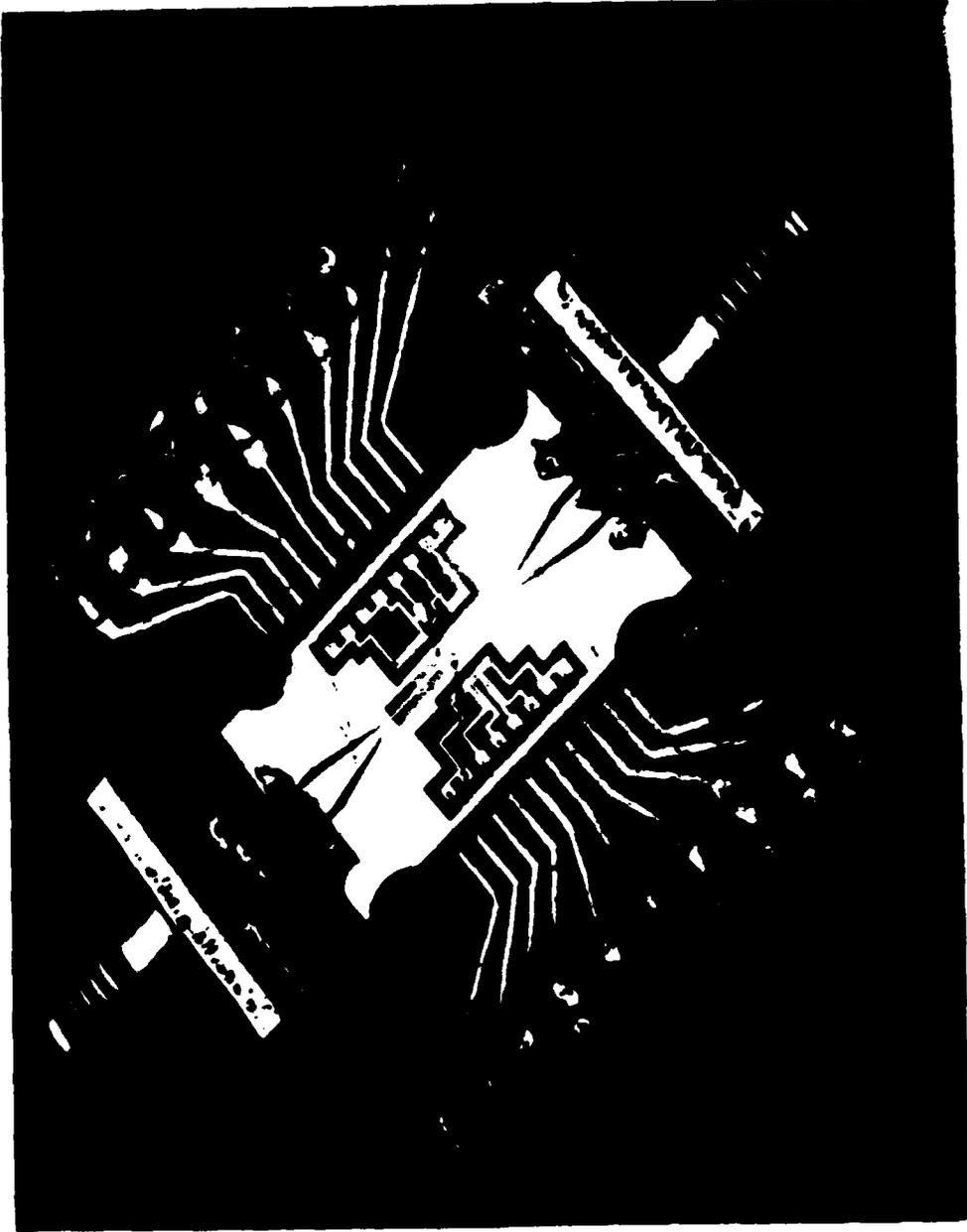
Figure 2. Photograph of SQUID VCO #3 mounted in the microwave holder. The two VCO's are connected to OSM connectors through the tapered 50 ohm coplanar lines with gold foil. DC leads are connected via wire-bonds to the adjacent connectors.
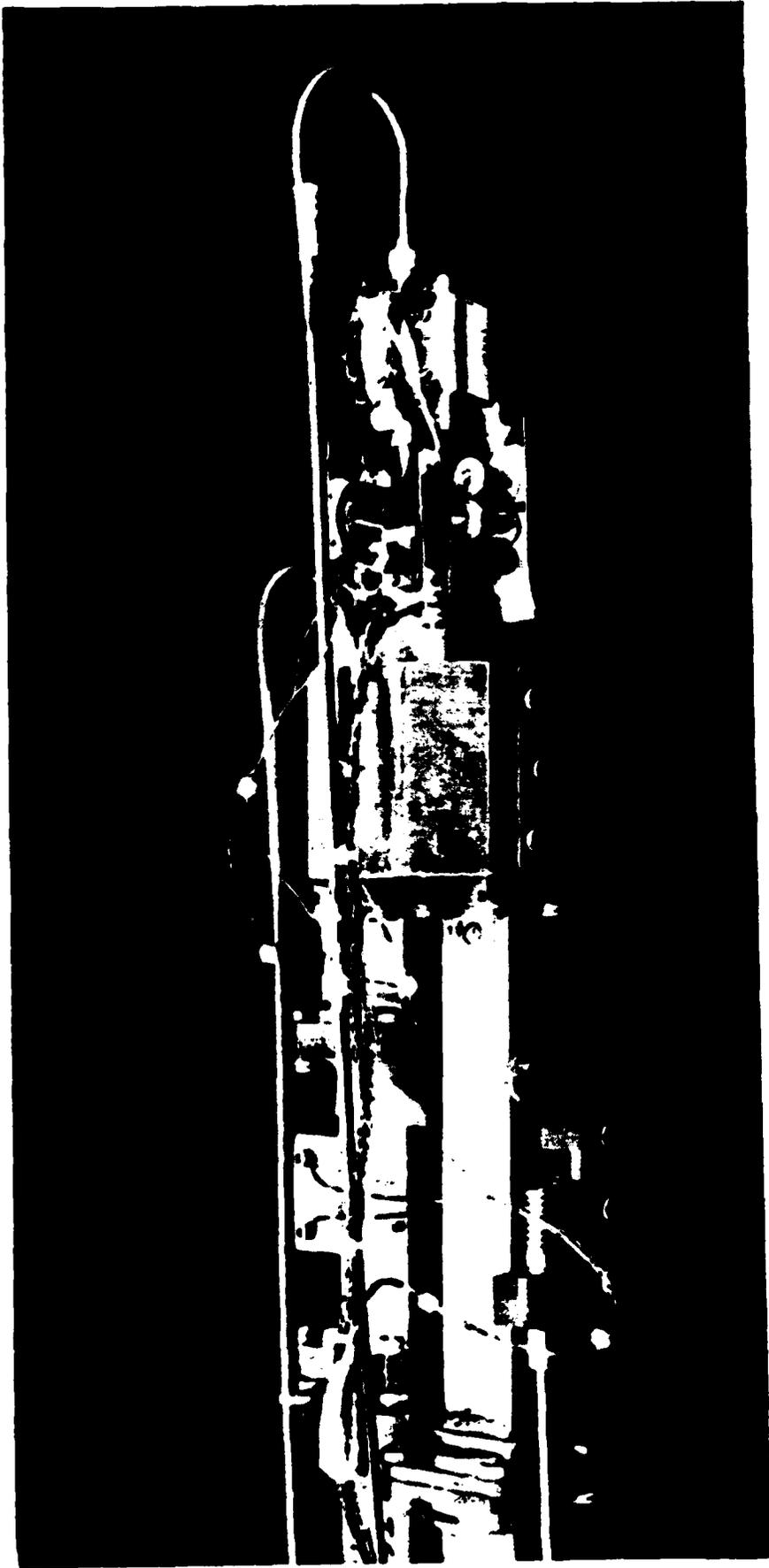
Figure 3. Photograph of the microwave probe assembly showing the stainless steel wave guides, cooled circulator, and sample assembly. A variable 30dB attenuator is in the upper waveguide to provide isolation from 300K noise in the input line. The entire assembly is immersed directly in LHe.
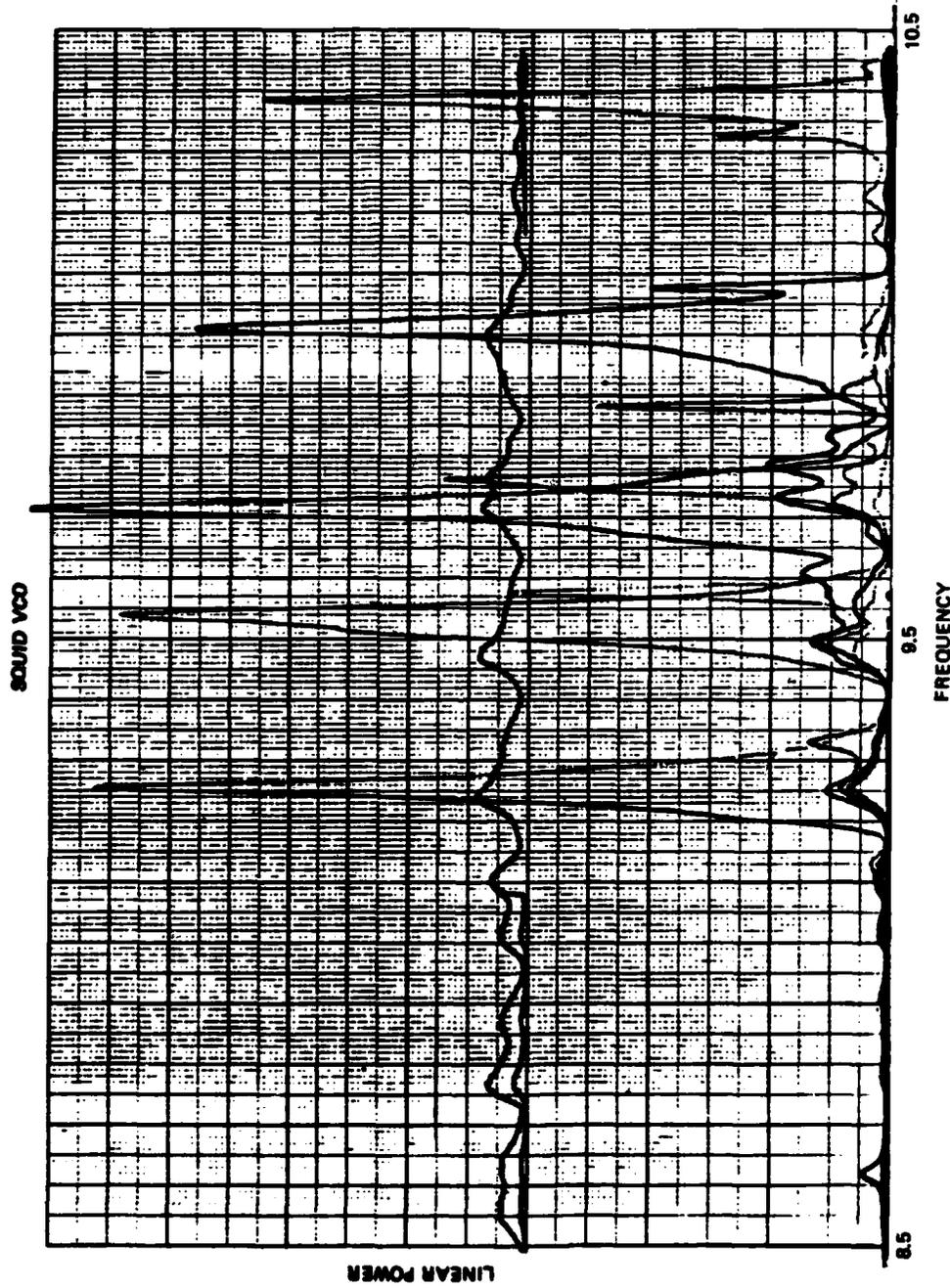
Figure 4. Recordings of the power spectra from VCO #3 measured by the spectrum analyzer with 300kHz bandwidth. The power scale is linear. The tracing near the center of the graph is the background response with the VCO in place but with no bias current.

9
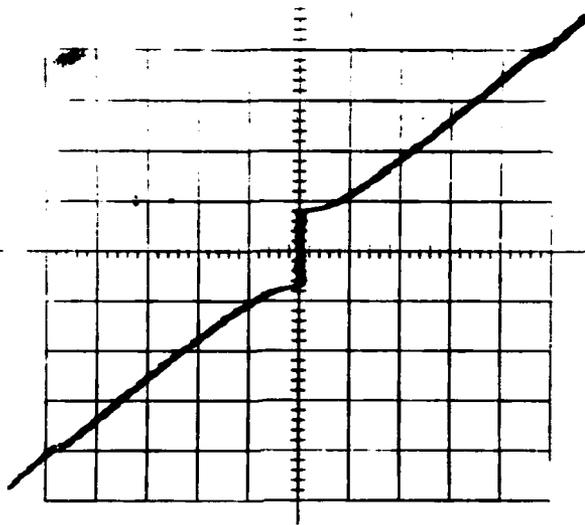
Figure 5. Current-voltage characteristic
of the voltage-clamped SQUID showing the
junction critical current and the nonhys-
teretic response of a 60mohm bias resis-
tance. The current scale (vertical) is
200 microamp/div and the voltage scale
(horizontal) is 10 microvolt/div.

dc SQUID COUPLING
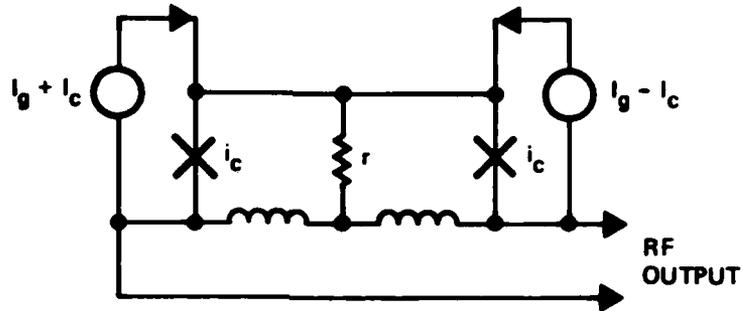
EQUIVALENT CIRCUIT
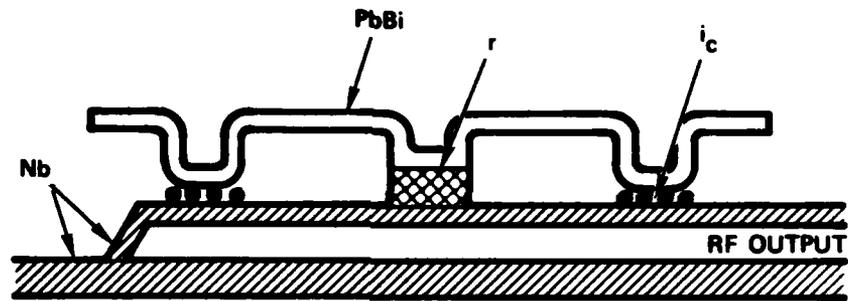
CROSS-SECTION VIEW

Figure 6. Diagram of the voltage-clamped dc SQUID VCO. The upper drawing is the equivalent circuit and the lower drawing is a vertical cross-section view of the device geometry. The lower two Nb films form a microstripline which is magnetically coupled to the SQUID inductance. The SQUID is fabricated on top of the microstripline.

11
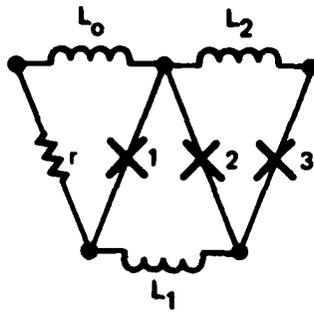
dc SQUID PAIR

EQUIVALENT CIRCUIT
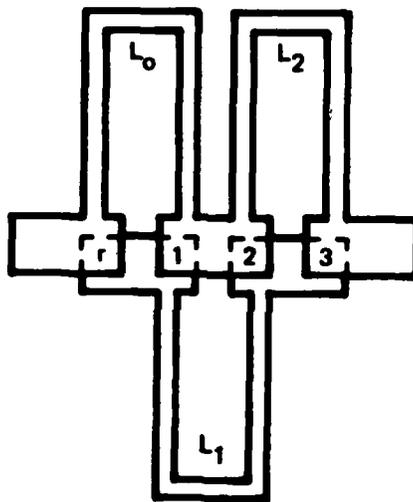
PLAN VIEW

Figure 7. Diagram of the voltage clamped dc SQUID pair. The voltage clamping is accomplished by a resistive SQUID which is junction-coupled to the dc SQUID pair. The upper figure is the equivalent circuit and the lower figure is a plan view of the device. This entire structure can be built above a ground plane or on a coupling microstrip.

EQUIVALENT
CIRCUIT

PLAN
VIEW

CROSS-SECTION
VIEWS
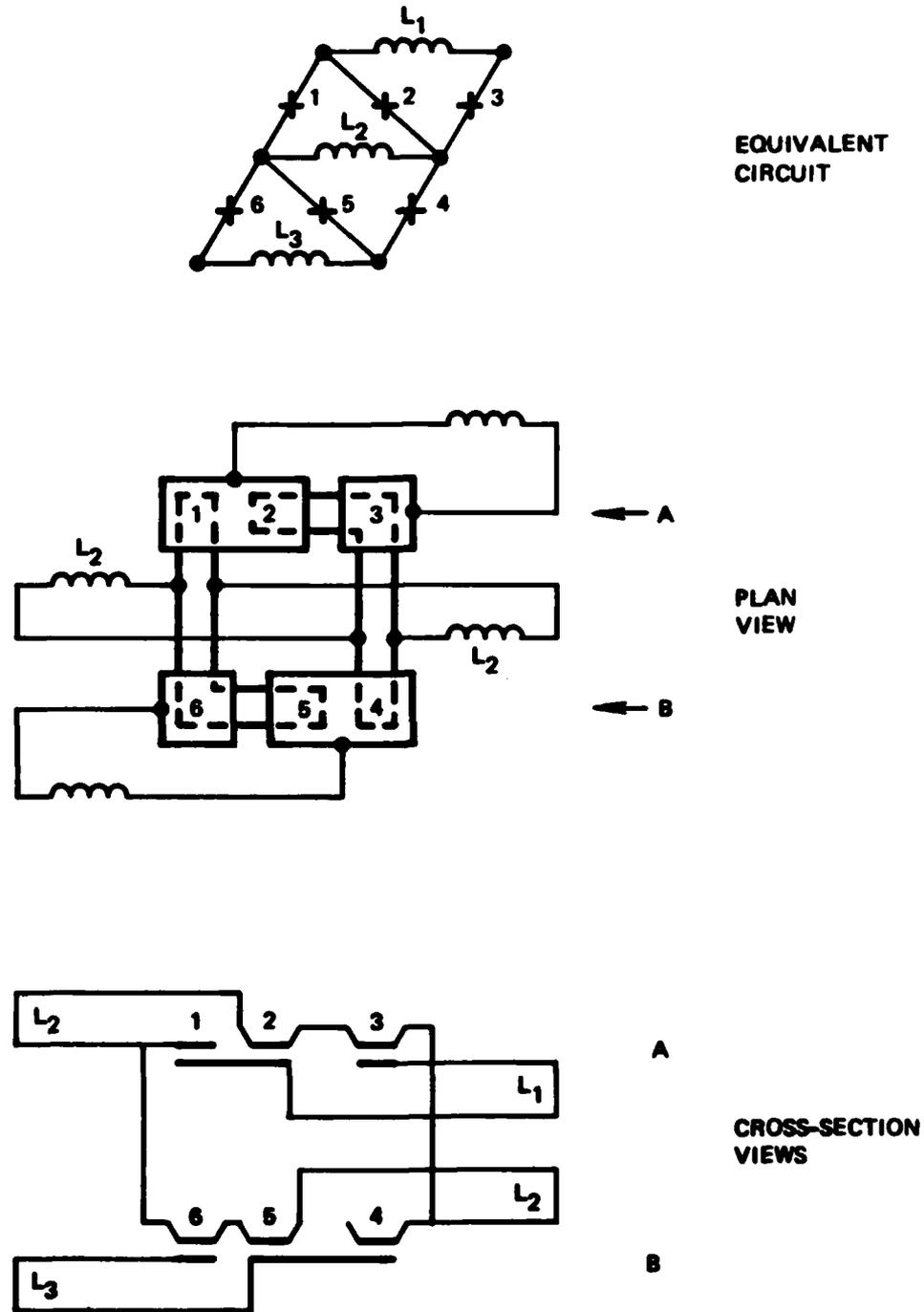
Figure 8.   Diagram of the Transverse flux-flow SQUID array.   A short array
equivalent circuit is shown at the top of the figure.   Plan and cross-section
views are shown below, with the numbering of the junctions and inductors
presented for clarity in interpereting the layout.   The cross-section views
A and B are displaced verically to permit unobstructed views.

13

SQUID VOLTAGE-CONTROLLED-OSCILLATOR*

A.H. Silver, R.D. Sandell, and J.Z. Wilcox
TRW Space and Technology Group
One Space Park, Redondo Beach, CA 90278

Abstract

We have investigated the SQUID as a voltage-controlled source of microwaves. The low impedance "resistive" SQUID can be a relatively high power ($\sim$nW), tunable, and monochromatic source for both on-chip and off-chip applications. Studies of the time-dependent junction phase and the available power spectra as they vary with such device parameters as loaded Q and the SQUID-$\beta = 2\pi L i_c/\phi_0$ establish design rules for a well-behaved oscillator. For a VCO $\beta Q < 2$; for $\beta Q > 2$ degenerate parametric subharmonic oscillations and chaotic instabilities are observed. Power increase is suggested by the use of voltage-clamped dc SQUIDs and arrays.

Introduction

The superconducting voltage-controlled-oscillator (VCO) has potential applications as an integrated, on-chip source for such superconducting devices as analog-to-digital converters (sampling clock), rf SQUID magnetometers (excitation source), parametric amplifiers (pump source), quasiparticle mixers (local oscillator), and intracomputer communications. A source of sufficiently high power can be useful as an agile signal generator. This paper describes the SQUID VCO as the implementation of this source.

The impetus for development of microwave/millimeter wave signal generators in superconducting technology has its origin in the Josephson relations which predict a sinusoidal Josephson current under the application of a dc voltage which is linearly related to the Josephson frequency, $\omega_J = 2\pi V/\phi_0$. Unfortunately, problems of impedance and the dynamics of the junction phase have made it difficult to achieve the expected performance.

We argue here that the SQUID and SQUID arrays are the natural forms for a VCO. In order to achieve linear tuning, the source resistance must be small compared to the junction impedance. Such a small resistance connected directly across the junction would short out the Josephson oscillations, greatly reduce the signal voltage across the junction, and no power will be delivered to the load. However, in a resistive SQUID (Fig. 1) the voltage-biasing resistor is isolated from the junction by the SQUID inductance L. Thus, the dc voltage will be developed across the bias resistor, the ac voltage across the inductance, and the total voltage across the junction.

Tunnel junctions generally have lower internal conductance than microbridges, at least below the energy gap, and are desirable junctions to minimize

internal losses. The shunt capacitance of the tunnel junction, which is frequently considered a serious shunting impedance, can be effectively parallel-tuned by the SQUID inductance. The load resistance, together with the internal junction resistance, will determine the loaded Q of the VCO.

One expects the instantaneous signal bandwidth to be determined by the Johnson noise across the net (low frequency) resistance as a result of frequency modulation of the oscillator by the thermal voltage fluctuations. This has been predicted and verified for point contact devices[1] as $\delta f = 4\pi k Tr/\phi_0^2 \approx 4.3\times10^7 rT$ for a biasing resistance r at temperature T. This value is independent of frequency to the extent that the bias current is stable and noise-free.

The stable operating mode of a low $\beta = 2\pi L i_c/\phi_0$ SQUID consists of regular flow of quantized flux ϕ_0. The internal circulating power in the SQUID is essentially that of changing quantized flux in the inductance L at the oscillation frequency, $P_{int} = \phi_0^2 \omega_J/4\pi L$, while the power delivered to the load resistance is V^2/R where $V = \phi_0 \omega_J/2\pi$. Thus, the power in the load is $P_R = P_{int}/\pi Q$ where $Q = R/\omega L$. Realistic values of L approximately 10^{-12}H project to $\sim 10^{-9}$W of power near 10GHz, with power increasing linearly with frequency at constant Q. This relation for P_R should be valid as Q decreases until the VCO is sufficiently loaded by R to reduce the ac voltage. Fundamental to achieving these power levels is small L and small Q. This requirement leads directly to load resistance values $R = Q\omega L$ of the order of $10^{-1}\Omega$ for $Q \sim 1$, $L \sim 10^{-12}$H, and $f_J \sim 10$GHz. Proper impedance matching is clearly necessary for both on-chip and off-chip applications. Coherent arrays of SQUIDs which will increase the total impedance can increase the available power as well as simplify the impedance matching.

Resistive SQUID

We have investigated the voltage-clamped SQUID in two forms: the resistive SQUID (Fig. 1a) and the dual resistive SQUID with common voltage-biasing resistor which we call the voltage-clamped dc SQUID (Fig. 1b). The dynamical response of the SQUID shown in Fig. 1a was simulated numerically to predict the operating characteristics of the SQUID VCO. We envision R to be the load to which power is delivered. This circuit obeys the relation

$$\ddot{\theta} + (\eta_R + \eta_I)\dot{\theta} + (1 + \eta_I\eta_R + \beta\cos\theta)\dot{\theta} + \eta_I\beta\sin\theta = \dot{\beta}_I + \eta_R\beta_I \quad (1)$$

where θ is the junction phase, $\eta_R = \sqrt{L/C}/R = Q^{-1}$, $\eta_I = r/\sqrt{L/C}$, $\beta = 2\pi L i/\phi_0$, $\beta_I = 2\pi L I/\phi_0$, and time is measured in $1/\omega_0 = \sqrt{LC}$. The voltage across the junction and load resistor R is $V = \phi_0 \omega_0 \dot{\theta}/2\pi$. The last term on the right hand side of Eq. (1) is approximately the expected Josephson frequency ω_J/ω_0 for $I \gg i_c$ and is equivalent to a voltage source (rI) in series with r; the actual dc voltage across the junction is somewhat lower than rI and must be determined by either direct measurement or calculation of $\langle\dot{\theta}\rangle$.

The simulations derived $\theta(t)$ and $\dot{\theta}(t)$ for selected values of η_I, η_R, β, and β_I with $\dot{\beta}_I = 0$. The results are essentially independent of η_I for all reasonable values of interest and so $\eta_I = 10^{-3}$ is used in all calculations reported here. This means that $I = 10^3 i_c$ and, hence, $\beta_I = 10^3$ at $\omega_J = \omega_0$.

The transient response is dominated by ω_0, Q and ω_J. Figure 2 shows the time evolution of θ and $\dot{\theta}$ for $\beta = 1$, $Q = 1$ and 5 for selected values of the voltage bias. For $Q = 1$, the turn-on transient is short
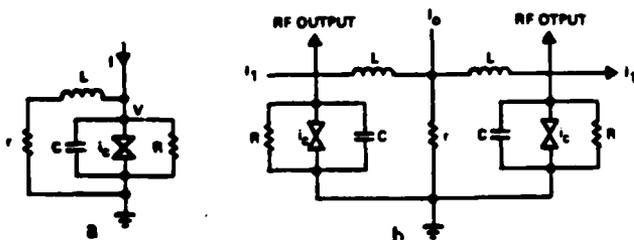
Figure 1. Equivalent circuit of SQUID VCO. (a) Resistive SQUID; (b) Voltage-clamped dc SQUID.
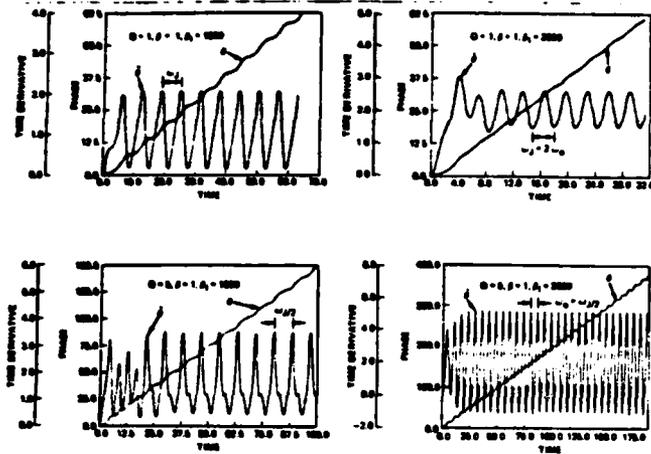
Figure 2. Selected transient response of θ and $\dot{\theta}$ for the resistive SQUID with $\beta=1$. Time is in units of ω_o^{-1}.

Figure 3. Q-dependence of the power delivered to the load at $\omega_J=\omega_o$ for $\beta=1$ in the resistive SQUID. Power is normalized to $[\omega_o\phi_o^2/(2\pi)^2 L]$.

(approximately Q/ω_o) and associated with shock excitation of the resonant LC circuit, the fundamental frequency of the periodic response is ω_J, and the periodicity in a smoothly stepped θ is 2π. If the Q is raised to 5, the transient reponse is longer and the resonance frequency becomes further involved with the oscillation. At $\omega_J/\omega_o=1.5$ ($\beta_I=1500$), there is a strong subharmonic component evident in the time response. At $\omega_J/\omega_o=2$ ($\beta_I=2000$), the response appears to be totally at $\omega_o=\omega_J/2$, while for Q=1 there was no evident subharmonic response. Generally, for either large β or large Q, the response becomes very complex and even aperiodic. The values required are not 100's, but of the order of 5. Even for smaller values, peculiarities occur somewhere in the spectrum if $\beta Q>2$.

In order to classify and quantify these measurements we have computed the power spectra for selected values of Q and β as a function of β_J. These were computed over 100 periods of the fundamental frequency of the oscillator after a long time interval after turn on, approximately 10^3 cycles. The Fourier amplitudes, including the dc value of $\langle\theta\rangle$, were calculated. The zero frequency amplitude was then compared to the fundamental frequency which was first calculated in establishing the time interval for the numerical integration. In general the fundamental frequency is $\langle\dot{\theta}\rangle=\omega_J/n$, except for anharmonic cases for which no fundamental frequency was found. Since the Fourier analysis was performed by a Fourier series no spectra were determined for anharmonic cases.

The power delivered to the load resistance R at any frequency is $P_i=V_i^2/R$ where V_i is the Fourier amplitude of the voltage at that frequency. The value computed numerically is $(\dot{\theta}_i^2/Q)$ which can be converted to physical units according to the relation

$$P_i = \omega_o\phi_o^2\dot{\theta}_i^2/(2\pi)^2 LQ. \qquad (2)$$

Figure 3 shows the dependence of the power delivered at ω_J for $\omega_J=\omega_o$ as a function of Q for $\beta=1$. The power has the expected maximum near Q=3, decreasing at high Q as Q^{-1} and at low Q because of loading of the SQUID. The maximum value of the power is approximately $1.124\ \phi_o^2\omega_o/(2\pi)^2 L$. For design values $\omega_o=2\pi\times9\times10^6$ and L=1pH, this corresponds to 12.9nW. However, as we have seen, values of Q>2 lead to some undesirable spectral response. Nevertheless, even for Q=1, the power is not even diminished by a factor of 2 from the peak value.

Figure 4 shows a compilation of the computed powers of the Josephson oscillations as a function of Q for $\beta=1$. In the regime Q<2, the spectra are well behaved except for a subharmonic response at $\omega_J=1.2\omega_o$, Q=2. For Q>2, there is a very strong subharmonic response at $\omega_J=2\omega_o$, and anharmonic response near $\omega_J=1.2\omega_o$. For $2<Q<5$, the region near $\omega_J=1.2\omega_o$ exhibits subharmonic behavior which is not plotted.
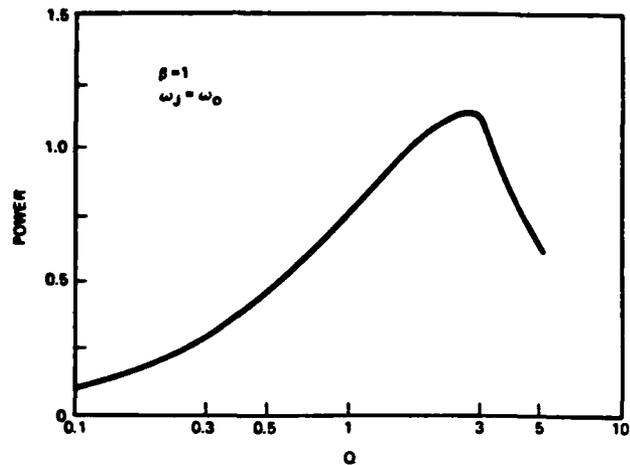
The strong subharmonic response when $\omega_J=2\omega_o$, which occurs at such modest Q's as 2.5, suggests degenerate parametric oscillations such as those predicted for the SQUID parametric amplifier[2]. This is also suggestive of the period-doubling effects reported to visit nonlinear systems such as Josephson junctions[3]. However, we also observe odd subharmonic responses for Q=5, $\beta=1$ which do not fall in the period-doubling class. An example of this is shown in Fig. 5 for Q=5, $\beta=1$, and $\beta_J=1100$.

These non-period-doubling subharmonics and the nonharmonic response occur in the general vicinity of $\omega_J=1.2\omega_o$ for Q=5, $\beta=1$; Levinson[4] has recently predicted odd-subharmonic response as the natural form of the instability in highly undamped Josephson junctions. For simulations which were conducted over a wide range of values of ω_J, the nonharmonic and odd-harmonic response is very localized in ω_J, although we only studied relatively small values of Q. Inspection of $\theta(t)$ suggests that θ spends relatively more time near $(2n+1)\pi$ in this regime, compared to $2n\pi$ for the more well-behaved regime. Since the junction is basically
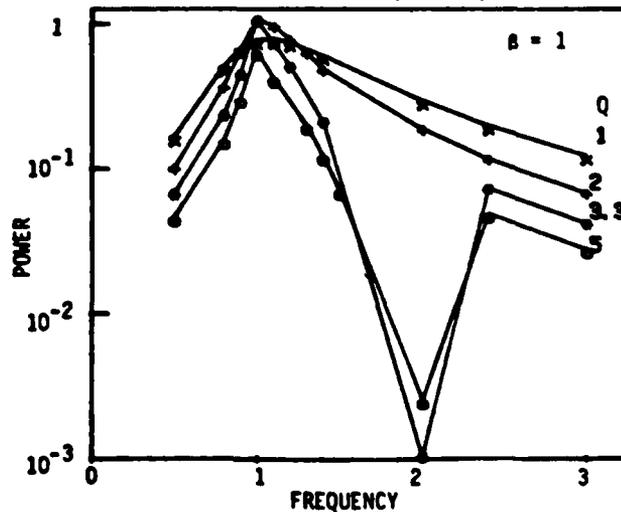
Figure 4. Frequency dependence of the power delivered to the load at ω_J for selected Q-values with $\beta=1$ in the resistive SQUID. Power is normalized to $[\omega_o\phi_o^2/(2\pi)^2 L]$.
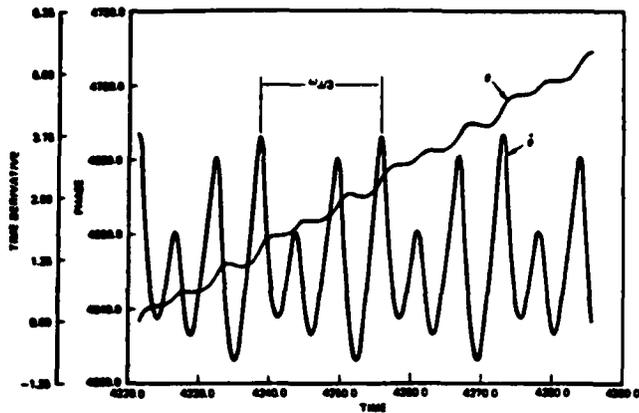
Figure 5. Computed transient response θ and $\dot{\theta}$ for the resistive SQUID with $\beta=1$, $Q=5$, and $\beta_1=1100$, corresponding to $\omega_J=1.1\omega_0$. Time is measured in ω_0^{-1}.

unstable for principal values $\pi/2 < \theta < -\pi/2$, this may be related to the instability.

The expected effect of increasing β at constant $Q=1$ is illustrated in the power spectra of Fig. 6. The bracketed symbols are the Josephson frequencies; the symbols connected by straight lines the predicted harmonics. Not all harmonic spectra are shown. Below $\beta=\pi$, all computed points are well behaved with some expected harmonics but no subharmonic response. For $\beta=\pi$, we observe subharmonics as we did for large Q values at $\beta=1$. For $\beta>\pi$, the time dependent response becomes even more complex and we have not computed spectral powers. Such β-values would be considered outside the normal range for a SQUID and moves toward the non-SQUID Josephson junction for which this analysis indicates very poor quality VCO.

Voltage-Clamped DC SQUID

The voltage-clamped dc SQUID of Fig. 1b can be recognized as a combination of two identical resistive SQUIDs with a common biasing resistor r. This leads to strong coupling of the two VCO's with identical frequencies but relative phases determined by the field current I_1. Two different modes of the coupled system are essentially a symmetric mode, with the two junctions in parallel, and an antisymmetric mode, with the two junctions in series. Maximum output power and impedance are achieved for the antisymmetric or series mode in which the circulating currents are in the same direction.
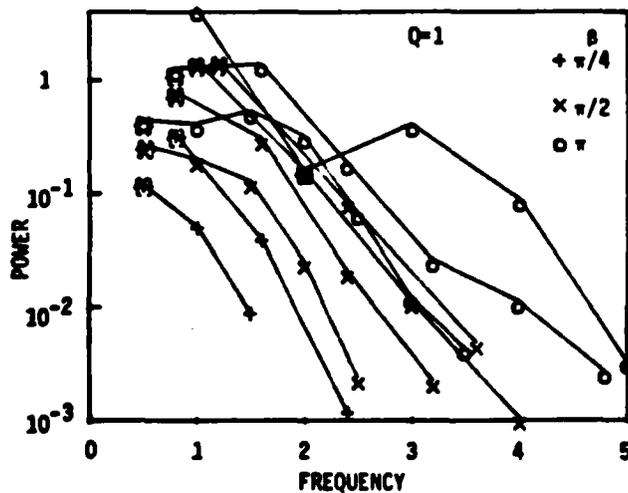
Figure 6. Harmonic spectra for the resistive SQUID with $Q=1$ and selected β.

We have carried out simulations of the symmetric voltage-clamped dc SQUID shown in Fig. 1b. The new parameters which define the device performance are $\beta_0=2\pi LI/\phi_0$, $\beta_1=2\pi LI_1/\phi_0$, $\theta_+=(\theta_R+\theta_L)/2$ and $\theta_-=(\theta_R-\theta_L)/2$. θ_R and θ_L refer to the phases of the right and left hand junctions, respectively, and we have defined β as $2\pi Li/\phi_0$, where L is the inductance of one-half of the dc SQUID. In a limited number of simulations with $\beta=1$ and $\beta_1=0$, the dc SQUID behaves identically to the resistive rf SQUID with $\theta_-=\theta=0$. The two junctions switch in-phase with one another and the resulting currents in each L add in the small resistance r. However, the voltage across the output (2L) is identically zero.

For $\beta_1=\pi/2$ and $\beta=1$, the computation shows that θ_- responds at the expected Josephson frequency while θ_+ responds at the second harmonic. This frequency doubling is a result of the alternate switching of the two junctions in each Josephson period. We have computed the response at $\beta_1=\pi/2$, $\beta=1$ for a range of Q from 1 to 5; the behavior of θ_- and θ_- is very similar to that observed for θ, θ in the resistive SQUID and will not be reproduced here.

SQUID Array VCO

Arrays of SQUIDs, driven coherently, can achieve further increase in power. Three types of arrays are possible: the longitudinal dc SQUID array, the transverse dc SQUID array, and the resistive SQUID bus. We discuss these briefly. Preliminary descriptions of the longitudinal and transverse dc SQUID arrays were given previously in connection with parametric amplification[2]. Figure 7 shows the simple circuits for both the linear dc SQUID arrays, and for a two-dimensional array which combines the two linear arrays. Analysis of the longitudinal flux-flow array has shown that it is unstable with respect to the flux-flow mode which is the one required for the VCO. As Sandell, et al[7] have shown, this type of array can provide series increase in rf impedance although it requires large dc currents because of its parallel nature at dc. Furthermore, in a tunnel junction implementation as compared with microbridges, narrow linewidths will require small biasing resistors as in the voltage-clamped dc SQUID. The transverse array is recognized as a series array of dc SQUID pairs. It provides increased impedance at both rf and dc, offering a reduction in the direct current required. Again, narrow linewidths will require small biasing resistors. It would be undesirable to fabricate large arrays requiring large numbers of carefully matched small resistors.

A method of avoiding the resistor network and producing a high power array is the resistive SQUID bus as shown in Fig. 7. It is an extension of the voltage-clamped dc SQUID to N resistive SQUIDs with a common voltage-biasing resistor. This could be readily accomplished in a thin film format with a pillbox resistor at the center of a radial array of SQUIDs. These might drive a coaxial line to an off-chip load.
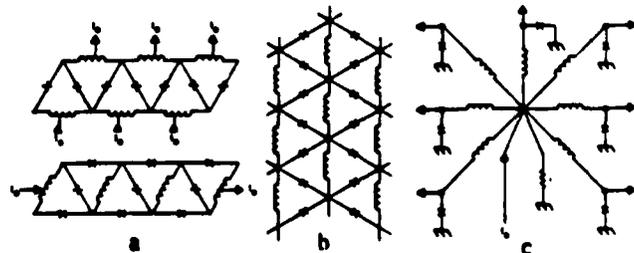
Figure 7. Schematic diagrams of SQUID arrays. (a) Longitudinal (upper) and transverse (lower) flux-flow arrays; (b) Two dimensional array; (c) SQUID bus.

On-chip, the bus can be used to drive many different loads which require coherent input, as in clocking a shift register or driving an array of mixers. If one supplies internal phase shifts of π between adjacent elements (as in the dc SQUID), then one can supply alternate out-of-phase signals. In either case, coherence is guaranteed by the common bias resistor and superconducting phase coherence.

Summary

The SQUID is the natural form for signal generation via the Josephson effect. While the bare Josephson junction suffers from both chaotic instabilities and low impedance, its incorporation in a low β, low Q SQUID tunes out the junction capacitance and controls the instability by directly harnessing the periodic nature of the junction phase to the quantum periodicity of the SQUID magnetic flux. This results in an efficient conversion of the Josephson energy to the circulating current in the SQUID inductance and, hence, to external circuitry. The power is maximized by minimizing the inductance, although at further reduction in source impedance. This last problem is alleviated by forming a priori coherent, stable arrays of SQUIDs to increase both the total power and impedance. Such arrays have the voltage-clamped dc SQUID as the basic cell. The design presented makes minimum demands on both lithography and Josephson current density.

Several experimental results have been reported in recent years which pertain to this device. The group at SUNY have studied microbridge VCO's, including pairs and arrays. The most successful results were in the dc SQUID-like arrays reminiscent of Fig. 7a, although the SQUID inductances were very large compared to the values suggested here. Calander and Zappe[8] proposed using a dc SQUID as a tunable oscillator for intracomputer communication in a Josephson processor[9]. They predicted $\sim 1\mu W$ of power at 500 GHz. Tuckerman[9] demonstrated this concept by connecting a dc SQUID transmitter with another dc SQUID receiver by a superconducting microstripline. The transmitted microwave signals were readily detected. Calander, et al[10] demonstrated a resistive SQUID VCO incidentally to their self-pumped Josephson parametric amplifier. Using a SQUID with $\beta=2$, L=3pH, $r=3\times10^{-2}\Omega$, and a 1Ω matching transformer, they observed 0.15nW at 10.4 GHz with a bandwidth of 150 MHz. This linewidth is much greater than the thermal-noise-limited value, 5 MHz, and is reportedly broadened by noise in the bias current. Assuming that the average power is diminished by the same factor as the line broadening, one could have expected as much as 4.5nW, in excellent agreement with the predictions of the model.

References

1. A.H. Silver, J.E. Zimmerman, and R.A. Kamper, "Contribution of Thermal Noise to the Linewidth of Josephson Radiation from Superconducting Point Contacts," Appl. Phys. Lett. 11, pp. 209-211 (1967).

2. A.H. Silver, D.C. Pridmore-Brown, R.D. Sandell, and J.P. Hurrell, "Parametric Properties of SQUID Lattice Arrays," IEEE Trans. Magn. MAG-17, pp.412-415 (1981).

3. R.L. Kautz, "The ac Josephson Effect in Hysteratic Junctions: Range and Stability of Phase Lock," J. Appl. Phys. 52, pp. 3528-3541 (1981); "Chaotic States of rf-Biased Josephson Junctions," J. Appl. Phys. 52, pp. 6241-6246 (1981).

4. M.T. Levinsen, "Even and Odd Subharmonic Frequencies and Chaos in Josephson Junctions: Impact on Parametric Amplifiers?," J. Appl. Phys. 53, pp. 4294-4299 (1982).

5. J.E. Zimmerman and A.H. Silver, "Coherent Radiation From High-Order Quantum Transitions in Small-Area Superconducting Contacts," Phys. Rev. Lett. 19, pp. 14-16 (1967).

6. A.H. Silver and J.E. Zimmerman, "Coupled Superconducting Quantum Oscillators," Phys. Rev. 158, pp. 423-425 (1967).

7. R.D. Sandell, C. Varmazis, A.K. Jain, and J.E. Lukens, "Flux Modulated Coherent Radiation from Arrays of Josephson Microbridges Coupled by Superconducting Loops," IEEE Trans. Magn. MAG-15, pp. 462-464 (1979).

8. N. Calander and H.H. Zappe, "Components for a Josephson Intracomputer Communication System," J. Appl. Phys. 50, pp. 3768-3769 (1979).

9. D.B. Tukerman, "Digital Frequency-Division Multiplexing Using Josephson Junctions," Thesis, MIT (1980).

10. N. Calander, T. Claeson, and S. Rudner, "Shunted Josephson Tunnel Junctions: High Frequency, Self-Pumped Low Noise Amplifiers," J. Appl. Phys. 53, pp. 5093-5103 (1982).

END

FILMED

11-83

DTIC